Journal of Materials Chemistry A

Accepted Manuscript

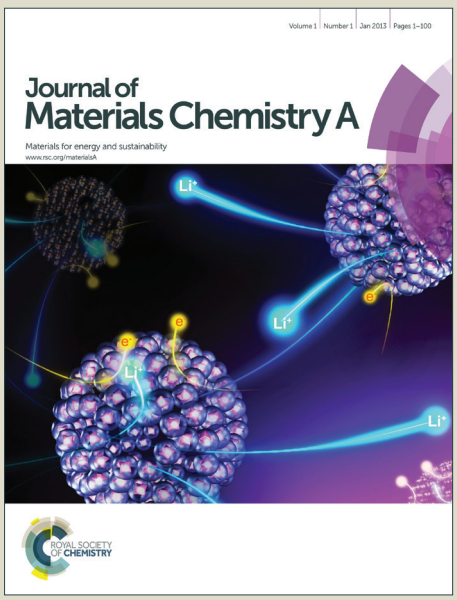

ROYAL SOCIETY OF CHEMISTRY

www.rsc.org/materialsA

Journal Name

COMMUNICATION

Design and Understanding of High-Performance Gas Sensing Material Based on Copper Oxide Nanowires Exfoliated from Copper Meshes Substrate

Received 00th January 20xx,
Accepted 00th January 20xx

DOI: 10.1039/x0xx00000x

www.rsc.org/

Fuchao Yang [ac], Jie Guo [ab], Mingming Liu [ac], Shen Yu [ab], Ningbo Yan[ad], Jing Li [a] and Zhiguang Guo*[ab]

We firstly reported a novel and facile route to synthesize 1D needlelike CuO gas sensor utilizing simple solution-treatment, heat-treatment and sonication process based on copper meshes (CM). We have demonstrated that the architectural 1D CuO sensor displays substantial improvement of response magnitude toward a series of toxic organic molecules. We expect that our work may provide a new inspiration for synthesizing 1D semiconductor nanowires for gas sensing application.

The elaboration and optimizing of gas sensors are present at the focus of collective research endeavours owing to the fact that it plays an ever-increasing role in outdoor or indoor environmental monitoring, assessment of food freshness, lung cancer detection, industrial surveillance and so on.[1-3] Transition metal oxides have emerged as a viable alternative in fabricating highly efficient gas sensors because they can provide ppm level sensitivity, fast response, low cost, low power, good selectivity and stability.[4,5] In particular, cupric oxide (CuO), as a p-type semiconductor with a narrow band gap of 1.2 eV, is considered as one of the most appealing inorganic materials for applications in chemical sensors because of its efficient catalytic activity, good electrochemical performance, and excellent surface adsorption property.[6-8] The CuO gas sensor material is usually made from copper salt, and we propose and demonstrate that it can be obtained by exfoliating from the as-designed copper meshes.

In recent years, the rational design and synthesis of one-dimensional (1D) nanostructures, such as nanowires,[9] nanoribbon,[10] nanotubes,[11] nanorods[12] and nanofibers,[8,13] have received extensive attentions because of their novel electrochemical properties related to larger surface area and more effective surface defect concentration as well as their potential advantages in catalysis, electronics, and gas sensors. There are various conventional methods applied to generate 1D nanostructural material, such as assisted by Pt in vacuum,[9] thermal deposition,[10] microwave-assisted hydrothermal method,[12] electrospinning,[13] *etc*. However, some limitations still remain in these approaches, including extremely high vacuum, superhigh temperature, extra-high voltage or other harsh growing conditions. It is quite desirable to develop a facile and versatile route for the controllable production of 1D functional nanomaterials under atmosphere without depending on any other complicated devices.

Herein, we demonstrated an interesting, simple, cost-effective and energy-saving strategy for preparing uniform 1D CuO nanowires, which possessed enhanced gas sensing properties. An air dry oven and a ultrasound equipment are all the devices we needed. In short, three steps are involved in this process as schematically shown in scheme 1: etching by alkaline solution, dehydrating by heat treatment and exfoliating by low-power sonication. To the best of our knowledge, this is the first report of CuO nanowires fabricated by this facile route

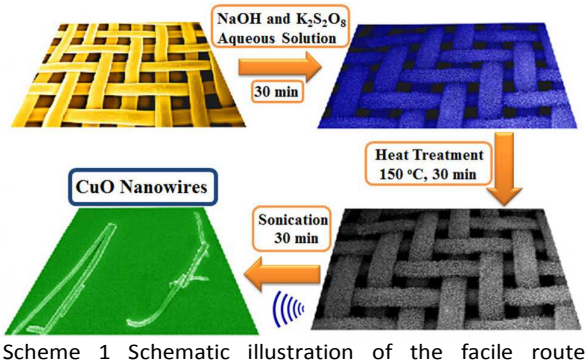

Scheme 1 Schematic illustration of the facile route involved three steps for the generation of CuO nanowires

[a] State Key Laboratory of Solid Lubrication, Lanzhou Institute of Chemical Physics, Chinese Academy of Sciences, Lanzhou 730000, People's Republic of China
[b] Hubei Collaborative Innovation Centre for Advanced Organic Chemical Materials and Ministry of Education Key Laboratory for the Green Preparation and Application of Functional Materials, Hubei University, Wuhan 430062, People's Republic of China
[c] University of Chinese Academy of Sciences, Beijing 100049, People's Republic of China
[d] School of Mechanical & Electrical Engineering, Wuhan Institute of Technology, Wuhan 430073, People's Republic of China

† Electronic Supplementary Information (ESI) available: Experimental procedure and figures S1-7. See DOI: 10.1039/x0xx00000x

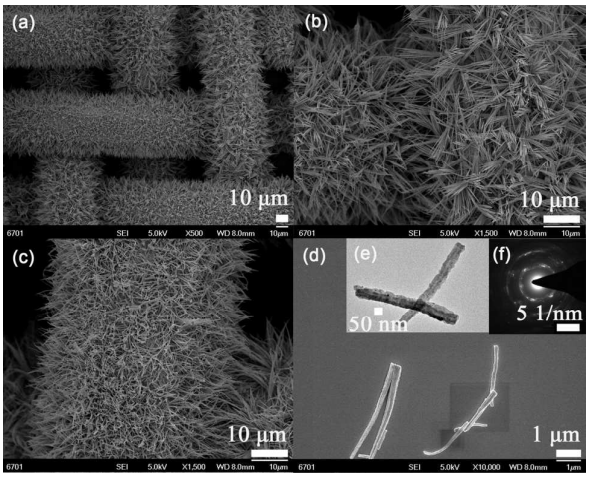

Fig.1 FESEM images of alkaline etching CM with low (a) and high (b) amplification, after 150 °C annealing (c), and the 1D CuO powder form (d). The inserts are TEM images of 1D CuO powder (e) and its corresponding electron diffraction pattern (f).

for use in gas sensing applications.

The surfaces of metals can often be finely oxidized and textured by mixed alkaline solution. [14, 15] In our experiment, the cleaned copper mesh (CM) was firstly put into the aqueous solution of 1.0 M NaOH and 0.05 M $K_2S_2O_8$ at room temperature for 0.5 h. After this process of sacrificial oxidation, the surface of CM was reconstructed by the needlelike structure (Fig.1a and b) and its colour turned to blue from shiny red (Fig.S1a-b, ESI). This alkali etching and oxidation process can be understood by the following chemical equation:

$$Cu + 2NaOH + K_2S_2O_8 \rightarrow Cu(OH)_2 + Na_2SO_4 + K_2SO_4 \quad (1)$$

The blue substance covering the CM was $Cu(OH)_2$ and further evidence will be shown later by X-ray diffraction (XRD), thermo-gravimetric analysis (TGA) and X-ray photoelectron spectra (XPS). The 1D nanowires CuO covering CM can be obtained by thermal decomposition of the needlelike $Cu(OH)_2$ at 150 °C in air, accompanying with the colour changing into black (Fig.S1c).

It is worth to note that the formed CuO inherit the 1D nanostructure from the needlelike $Cu(OH)_2$, as shown in Fig.1c. The transformation of $Cu(OH)_2$ into CuO in the solid state by thermal dehydration often generate the reserved morphology while the transformation take place in solution usually accompanies a morphological change.[16] The CuO was successfully detached from the CM substrate utilizing sonication. The morphology of CuO powder form was obtained by dropping its dispersion on the Si substrate, which was given in Fig.1d. Several CuO nanorods lie on the substrate and its 1D nanostructure was not destroyed during the sonication process. After 30 min sonication, the FESEM images of the residual CM were given in Fig.S2. Transmission electron microscopy (TEM) was also employed to characterize its detailed structures, exhibiting highly dispersed nanowires morphology (Fig.1e). The diameters of these CuO nanowires were probably estimated

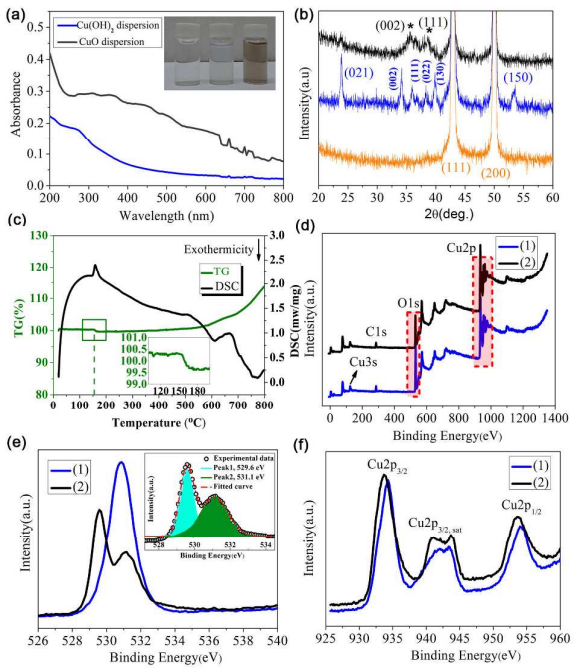

Fig.2 (a) UV-visible absorption spectra and photograph (inset, the left vial show background) of $Cu(OH)_2$ and CuO ethanol dispersion (b) XRD patterns of original, after alkali etching, and after alkali etching and annealing CM (c) TGA curve indicates the transition process from $Cu(OH)_2$ into CuO covering CM. The XPS full spectrum (d) and the XPS O1s (e) and Cu2p fine spectrum (f) of CM covered by blue (1) and dark (2) substance.

to be 50-70 nm (65%, Fig.S3a in ESI) and the selected area electron diffraction pattern exhibit polycrystalline rings, indicating that the 1D product is composited of polycrystalline CuO (Fig.1f and Fig.S3b).

In Fig.2a, we provide the photograph (insert) and UV-vis absorption spectra of $Cu(OH)_2$ and CuO ethanol dispersion. Compared with the pure ethanol given as blank control (left), $Cu(OH)_2$ (middle) and CuO (right) ethanol dispersion show light blue and brownish black. Both these two absorption spectra show much higher absorption in the UV region (200-400 nm) than visible region (400-800 nm). The $Cu(OH)_2$ ethanol dispersion show blue colour which indicate that it would absorb the visible light with particular colour of wavelength and other can pass. In other words, it selectively absorbs the complementary orange-red light (650-760 nm). Several absorption peaks among this region can be found in its partial enlarged drawing, provided as Fig.S4 in ESI. As for CuO ethanol dispersion, it absorbs strongly throughout the visible spectrum and thus shows a brownish black colour. Spectroscopic analysis gives us a deeper insight into the observed color.[17] The holistic view XRD patterns of CM, $Cu(OH)_2$ or CuO covering CM exhibit similar (111) dominated diffraction peaks and the difference was beyond distinction as shown in Fig.S1e, ESI. Fig. 2b shows the enlarged XRD

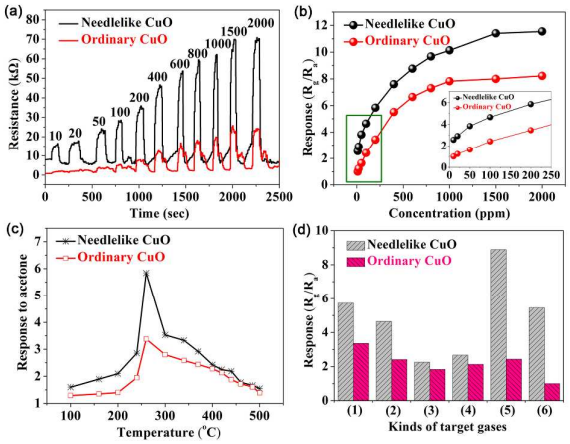

Fig.3 Dynamic resistance change curves (a) and the corresponding response value (b) of the CuO sensors to acetone of different concentrations. (c) The response of CuO sensors to 200 ppm acetone at different testing temperatures (d) Responses of CuO sensors to different target gases (100 ppm) at 260 °C.

patterns of CM, $Cu(OH)_2$ (blue line) or CuO (dark line) covering CM. Strong diffraction peaks from the CM substrate are also detected. The diffraction peaks of blue pattern correspond well with orthorhombic $Cu(OH)_2$ (Space group Cmcm(63), JCPDS 35-0505), which is consistent with the published paper.[18] The diffraction peaks marked with black asterisk can be indexed to monoclinic CuO (JCPDS 45-0937) and similar patterns have been reported by previous works.[19,20] It is reported that $Cu(OH)_2$ precursor precipitates transform itself into CuO particles after heat treatment at 90 °C for 12 h.[18] To well understand the thermal conversion process in our experiment, TGA was performed and the sample measurement was taken under air atmosphere from room temperature to 800 °C at a speed of 10 °C/min. At about 150 °C, the blue $Cu(OH)_2$ covering on CM show a stage weight loss pattern (decreasing of mass by 1%, the insert of Fig.2c) evidently, resulting from the conversion of $Cu(OH)_2$ into CuO. It is rationally believed that the sharp increase of weight at about 600 °C is attributed to the conversion of part CM substrate into CuO. In Wang's work, they studied the conversion of $Cu(COOC_6H_4NH_2)_2$ films into CuO/C composite films using the same analytic approach.[20] Fig. 2d-f shows the XPS full spectrum, O1s and Cu 2p fine spectra obtained from CM covered by blue or dark colour substance. The related peaks of Cu3s, C1s, O1s and Cu 2p were detected and centred at the binding energy of 124.1, 285.1, 530.1, and 930-960 eV, correspondingly. In Fig. 2e, the dark line spectra of high-resolution core level of the O 1s state shows a broad asymmetric curve which can be fitted into two Gaussian peaks: a peak at 529.6 eV indicating O^{2-} bonded with Cu^{2+} and the second peak at 531.1 eV indicating surface adsorbed oxygen on CuO nanowires. The above results are in full accordance with the previous report.[21] In the characteristic high-resolution spectrum of Cu 2p, it was split into Cu $2p_{3/2}$, Cu $2p_{3/2,\ sat}$ and Cu $2p_{1/2}$ peaks. The Cu $2p_{3/2}$ peak raised from $Cu(OH)_2$ is centred at 934.28 eV while that of CuO locates at 933.68 eV. This analysis and variation tendency is accordance with Lee and coworkers.[22] Moreover, the two extra shake-up satellite peaks raised from CuO were evidently observed at 941.08 and 943.68 eV, which indicates the presence of an unfilled Cu $3d^9$ shell and thus further confirming the presence of CuO.[21, 23] The Cu $2p_{1/2}$ peak raised from $Cu(OH)_2$ is centred at 954.08 eV while that of CuO locates at 953.58 eV, which indicates that both Cu $2p_{3/2}$ and Cu $2p_{1/2}$ peaks shift toward lower binding energy after heat treatment.

To illustrate the excellent gas sensing performances of the as-prepared needlelike CuO, we also investigated the gas-sensing property of ordinary CuO in a comparative view. In briefly, the synthetic method of ordinary CuO was directly mixed the aqueous solutions of $CuSO_4{\cdot}5H_2O$ and NaOH, and endured the annealing process just as the condition of needlelike CuO. The ordinary CuO exhibits spindle-like shape with a width of 50 - 200 nm. Its synthetic details and characterizations were given in ESI. The gas sensing tests were performed under the condition of relative humidity at about 22 % and environment temperature at about 18 °C. As clearly shown in Fig.3a, all these two sensors showed typical p-type gas sensing behavior, i.e., an increase in resistance on reducing gases.[24] The gas sensing performances of needlelike CuO were greatly enhanced and independent of the concentrations of acetone. The corresponding response values can be calculated based on R_g/R_a and the results were given in Fig.3b. As for 50 ppm, the response value of needlelike CuO sensor is 3.82, which is about 2.3 times as that of ordinary CuO sensor (1.64). As for 100 ppm, the response value of needlelike CuO sensor is 4.64, which is about 1.9 times as that of ordinary CuO sensor (2.41). The curves exhibit that the response values increase rapidly when the concentration is lower than 800 ppm. But when the concentration is over 800 ppm, the increase rate become slow, indicating that the sensor is more or less statured.[25] Fig. 3c shows the responses of needlelike and ordinary CuO sensors to acetone of 200 ppm as a function of the operating temperature. The sensors of needlelike and ordinary CuO exhibit the highest response to acetone gas at 260 °C. In general, it is also observable in Fig. 3c that the sensitivity values increase remarkably at first and then degrade dramatically with the increase of working temperature. Combining the catalytic role of CuO with the unique characteristics of 1D microstructure, we expect that the as-synthesized needlelike CuO can be promising candidates for high performance gas sensors to detect some chemical contaminants and dangerous gases, i.e., ethanol (1), acetone (2), benzene (3), toluene (4), benzaldehyde (5) and benzyl alcohol (6). The concentration of these gases is 100 ppm, being conducted at 260 °C. As demonstrated in Fig. 3d, the needlelike CuO sensor is superior to ordinary CuO sensor for all kinds of these target analytes. The needlelike CuO sensor show excellent selectivity to benzaldehyde (8.89), which is about 4 times as that of sensitivity to benzene (2.25).

The metrics of gas sensors require high response magnitude and fast rate. The fast rate here regard gas sensors on going for a relatively rapid switching capabilities when it was exposed to

or released the target gas.[26] The method for obtaining response time (T_s) and recovery time (T_c) are given in ESI, which are further illustrated by Fig. 4a-b. As it is shown, the T_s and T_c of needlelike CuO sensor to 1 ppm acetone is 96.6 s and 19.1 s. The T_s and T_c of needlelike CuO sensor to 10 ppm acetone is 52.6 and 22.9 s. These response and recovery time are acceptable for practical application.[1,26] While it is hard to obtain the T_s and T_c of ordinary CuO sensor to acetone at this low ppm level, its response and recovery behavior are submerged by noise signal when the sensing curves are magnified. The response and recovery behaviors of needlelike CuO sensor to benzene, benzaldehyde and benzyl alcohol are also investigated and are provided as Fig.S6 in ESI. For a utility-type gas sensor, the reproducibility and long-term stability are also important issues. The reproducibility of needlelike CuO sensor is studied through repetitive injecting or releasing the 5 ppm acetone over several times. Fig.4c shows the results that the peaks and valleys are found nearly constant, suggesting that the reliability of needlelike CuO sensor. The reproducibility of needlelike CuO sensor to 100 ppm ethanol and benzene was also studied and was given in Fig.S7b (ESI). The long-term stability of the sensors was measured to 100 ppm acetone for a month and the response value of initial, after 15-days and after 30-days is 4.64, 4.31 and 4.24 as shown in Fig. 4d, which confirms the long-term stability of the sensor by our measurement.

Finally, we discuss the mechanisms that can lead to a resistance change in needlelike CuO sensor upon interaction with analytes, as shown in Fig.4e. When our sensor exposed to air, the chemisorbed oxygen ions (O_2^-, O^- and O^{2-}) are formed on the surface of CuO by capturing electrons from its surface.[27,28] The concentrations of adsorbed oxygen species (O_2^-, O^- and O^{2-}) are largely depended on the operating temperatures, specific surface area and surface active centers.[2,28] The 1D nanostructure often exhibits larger specific surface area and sufficient surface active centers.[4,5] When our sensors are exposed to reducing gases (six kinds of volatile gases in our experiment), these organic gas molecules are oxidized by oxygen species (O_2^-, O^- and O^{2-}), and simultaneously the electrons are fed back into CuO sensor body, leading to a recombination of electron and hole and thus causing a depletion of holes. As is well known, the conductive ratio of p-type semiconductor is greatly influenced by the concentration of the holes and so an increased resistance in needlelike CuO sensor is observed. According to the previous literatures,[24, 29] metal oxides with acidic (e.g., SnO_2 and WO_3), amphoteric (e.g., Fe_2O_3 and ZrO_2), and basic (e.g., CuO and La_2O_3) surfaces involve different interaction procedures and different sensing behaviors. Under basic conditions, the functional group of aldehydes (-CHO) is much more active than the alcohols and hydrocarbons.[24,27] Hence, benefiting from the surface basicity, a higher sensing response to benzaldehyde is observed.

In summary, we reported a simple solution-based method for the preparation of 1D needlelike $Cu(OH)_2$ and it conversion into the morphology reserved CuO gas sensor after heat treatment and sonication process. Consequently, the gas sensing performances of needlelike CuO were greatly enhanced. The response value of needlelike CuO sensor to 50 ppm acetone is about 2.3 times as that of ordinary CuO sensor. The needlelike CuO sensor show excellent selectivity to benzaldehyde, which is about 4 times as that of sensitivity to benzene. The T_s and T_c of needlelike CuO sensor to 1 ppm acetone is 96.6 and 19.1 s. The reproducibility and long-term stability of the needlelike CuO sensor were also demonstrated. We anticipate that our work may provide a new facile strategy for synthesizing metallic oxide semiconductor nanowires based on metal substrates for gas sensing application.

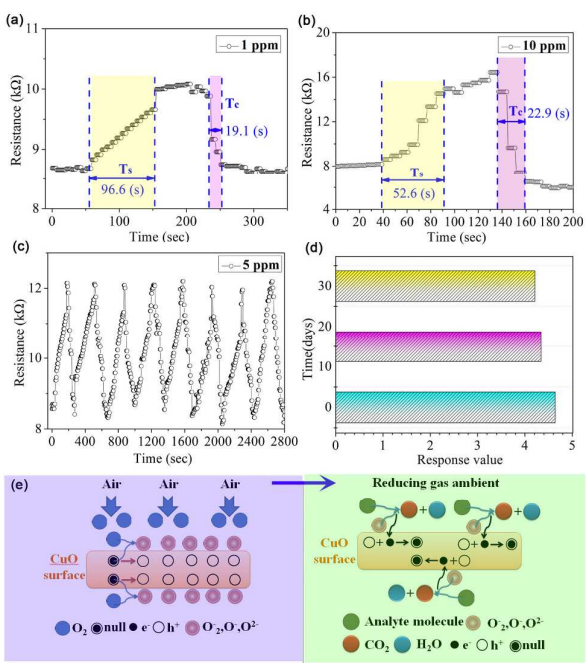

Fig.4 The transient response–recovery curves of needlelike CuO sensor to 1 ppm (a) and 10 ppm (b) acetone. (c) The reproducibility of needlelike CuO sensor to 5 ppm acetone. (d) Stability of needlelike CuO sensor to 100 ppm acetone over 30 days. (e) Schematic illustration for oxygen chemisorption and gas sensing mechanism.

Acknowledgements

This work is supported by the National Nature Science Foundation of China (Nos. 11172301 and 51522510), the "Funds for Distinguished Young Scientists" of Hubei Province (No. 2012FFA002), the "Western Light Talent Culture" Project, the Co-joint Project of Chinese Academy of Sciences, the "Top Hundred Talents" Program of Chinese Academy of Sciences and the National 973 Project (2013CB632300) for financial support.

Notes and references

1 J. R. Stetter and J. Li, *Chem. Rev.,* 2008, **108**, 352−366.
2 Y. J. Yun, W. G. Hong, N. J. Choi, H. J. Park, S. E. Moon, B. H. Kim, K. B. Song, Y. Jund and H. K. Lee, *Nanoscale,* 2014, **6**, 6511-6514.
3 A. Ziyatdinov, J. Fonollosa, L. Fernández, A. G. Gálvez, S. Marco and A. Perera, *Sens. Actuators B,* 2015, **206**, 538–547.
4 Y. S. Wang, S. R. Wang, H. X. Zhang, X. L. Gao, J. D. Yang and L. W. Wang, *J. Mater. Chem. A,* 2014, **2**, 7935–7943.
5 S. M. Niu, Y. F. Hu, X. N. Wen, Y. S. Zhou, F. Zhang, L. Lin, S. H. Wang and Z. L. Wang, *Adv. Mater.* 2013, **25**, 3701–3706.
6 Z. Y. Wang, Y. Xiao, X. B. Cui, P. F. Cheng, B. Wang, Y. Gao, X. W. Li, T. L. Yang, T. Zhang and G. Y. Lu, *ACS Appl. Mater. Interfaces,* 2014, **6**, 3888−3895.
7 C. Yang, F. Xiao, J. D. Wang and X. T. Su, *Sens. Actuators B,* 2015, **207**, 177–185.
8 A. Katoch, S. W. Choi, G. J. Sun, H. W. Kim and S. S. Kim, *Nanotechnol.,* 2014, **25**, 175501.
9 V. Gurylev, C. C. Wang, Y. C. Hsueh and T. P. Perng, *CrystEngComm.,* 2015, **17,** 2406-2412.
10 M. Law, H. Kind, B. Messer, F. Kim and P. D. Yang, *Angew. Chem. Int. Ed.,* 2002, **41**, 2405-2408.
11 A. Patole and G. Lubineau, *Carbon*, 2015, **81**, 720 -730.
12 C. Yang, X. T. Su, F. Xiao, J. K. Jian and J. D. Wang, *Sens. Actuators B,* 2011, **158**, 299–303.
13 S. Xu, K. Kan, Y. Yang, C. Jiang, J. Gao, L. Q. Jing, P. K. Shen, L. Li and K. Y. Shi, *J. Alloys Compd.,* 2015, **618**, 240–247.
14 Z. G. Guo, F. Zhou, J. C. Hao and W. M. Liu, *J. Am. Chem. Soc.,* 2005, **127**, 15670-15671.
15 C. A. Dai, N. Liu, Y. Z. Cao, Y. N. Chen, F. Lu and L. Feng, *Soft Matter*, 2014, **10**, 8116–8121.
16 Y.H. Liu, J. F. Mao, P. Jiang, Z. M. Xu, H.Y. Yuan and D. Xiao, *CrystEngComm*., 2009, **11**, 2285–2287.
17 X. C. Shan, F. L. Jiang, L. Chen, M. Y. Wu, J. Pan, X. Y. Wan and M. C. Hong, *J. Mater. Chem. C,* 2013, **1**, 4339–4349.
18 J. Y. Xiang, J. P. Tu, L. Zhang, Y. Zhou, X. L. Wang and S. J. Shi, *Electrochim. Acta,* 2010, **55**, 1820–1824.
19 Y. Lu, H. L. Yan, K.W. Qiu, J. B. Cheng, W. X. Wang, X. M. Liu, C. C. Tang, J. K. Kime and Y. S. Luo, *RSC Adv.,* 2015, **5**, 10773-10781.
20 H. B. Wang, Q. M. Pan, J. W. Zhao and W. T. Chen, *J. Alloys Compd.,* 2009, **476**, 408–413.
21 S. Das, S. Saha, D. Sen, U. K. Ghorai and K. K. Chattopadhyay, *Dalton Trans.,* 2015, **44**, 6098–6106.
22 M. Y. Lee, S. J. Ding, C. C. Wu, J. Peng, C.T. Jiang and C.C. Chou, *Sens. Actuators B,* 2015, **206**, 584–591.
23 M. Yin, C.K. Wu, Y. Lou, C. Burda, J. T. Koberstein, Y. Zhu and S. O'Brien, *J. Am. Chem. Soc.,* 2005, **127**, 9506–9511.
24 Z. F. Dai, C. S. Lee, B.Y. Kim, C. H. Kwak, J.W. Yoon, H. M. Jeong and J.H. Lee, *ACS Appl. Mater. Interfaces,* 2014, **6**, 16217−16226.
25 L. Xu, R. Q. Xing, J. Song, W. Xu and H.W. Song, *J. Mater. Chem. C,* 2013, **1**, 2174–2182.
26 J. Kong, N. R. Franklin, C.W. Zhou, M. G. Chapline, S. Peng, K. Cho and H. J. Dai, *Science,* 2000, **287**, 622-625.
27 M. Rumyantseva, V. Kovalenko, A. Gaskov, E. Makshina, V. Yuschenko, I. Ivanova, A. Ponzoni, G. Faglia and E. Comini, *Sens. Actuators B,* 2006, **118**, 208−214.
28 F.C. Yang and Z.G. Guo, *J. Colloid Interface Sci.,* 2015, **448**, 265–274.
29 N. Hosseinpour, A. A. Khodadadi, A. Bahramian and Y. Mortazavi, *Langmuir,* 2013, **29**, 14135−14146.

Table of contents

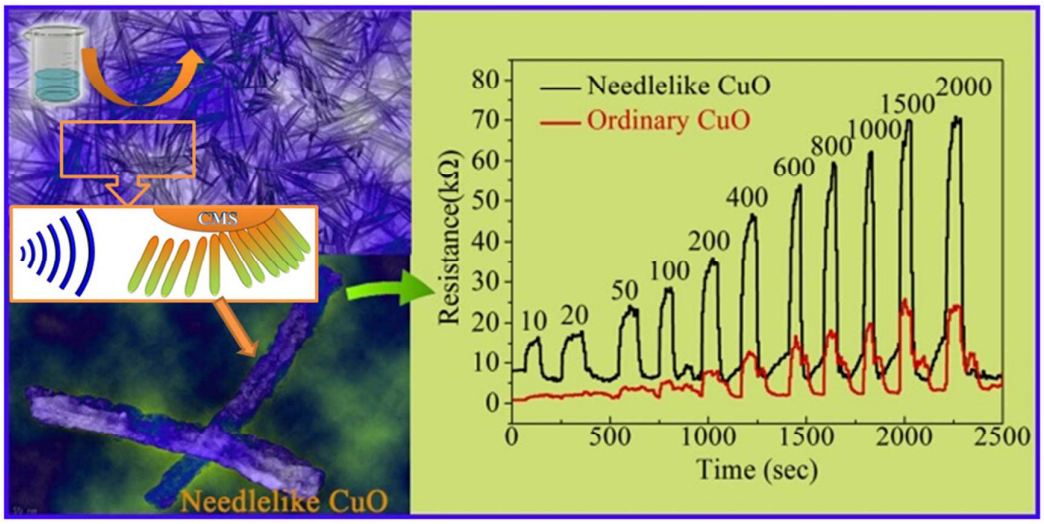

High-Performance Gas Sensing Based on Copper Oxide Nanowires Exfoliated from Copper Meshes Substrate (CMS).